

Decrease in NMDAR-NR2B subunit levels by intrathecal shRNA blocks group I mGluR-mediated hyperalgesia

Bichoy H. Gabra, Fay K. Kessler, Joseph K. Ritter, William L. Dewey and Forrest L. Smith

Department of Pharmacology and Toxicology, Virginia Commonwealth University Medical Center, Richmond, Virginia (*B.H.G., F.K.K., J.K.R., W.L.D.*); and Department of Pharmaceutics, College of Pharmacy, Harding University, Searcy, Arkansas (*F.L.S.*)

a) Running Title: The role of NMDA-NR2B subunit in mGluR-induced hyperalgesia

b) Author for correspondence:

William L. Dewey, Ph.D.

Department of Pharmacology and Toxicology, Virginia Commonwealth University Medical Center

P.O. Box 980613

Richmond, VA 23298-0613

Office: 804-827-0375

Fax: 804-827-1548

E-mail: wdewey@vcu.edu

c) Number of text pages: 26 pages

Number of tables: 1 table

Number of figures: 6 figures

Number of references: 40 references

Number of words in the *Abstract*: 224 words

Number of words in the *Introduction*: 712 words

Number of words in the *Discussion*: 1225 words

d) Abbreviations: NMDA, *N*-methyl-D-aspartic acid; NMDARs, *N*-methyl-D-aspartic acid receptors; AMPA, alpha-amino-3-hydroxy-5-methyl-4-isoxazolepropionic acid; NR1, NMDA-R1 subunit; NR2, NMDA-R2 subunit; NR3, NMDA-R3 subunit; mGluRs, metabotropic glutamate receptors; PKC, protein kinase C; PKA, protein kinase A; PKG, protein kinase G; AMP, adenosine monophosphate; (*S*)-3,5-DHPG, (*S*)-3,5-dihydroxyphenylglycine; (*S*)-4C3HPG, (*S*)-4-carboxy-3-hydroxyphenylglycine; MPEP, 2-

methyl-6-(phenylethynyl)-pyridine; 3-MATIDA, α -amino-5-carboxy-3-methyl-2-thiopheneacetic acid; CGS 19755; *cis*-4-[phosphomethyl]-piperidine-2-carboxylic acid; CGP 78608, [(1*S*)-1-[(7-bromo-1,2,3,4-tetrahydro-2,3-dioxo-5-quinoxaliny)methyl]amino]ethyl]phosphonic acid; Ro 25-6981, [R-(R*,S*)]- α -(4-Hydroxyphenyl)- β -methyl-4-(phenylmethyl)-1-piperidinepropanol hydrochloride; Go-7874, 12-(2-Cyanoethyl)-6,7,12,13-tetrahydro-13-methyl-5-oxo-5H-indolo(2,3-a)pyrrolo(3,4-c)-carbazole; PKI-(14-22)-amide, Myr-N-Gly-Arg-Thr-Gly-Arg-Arg-Asn-Ala-Ile-NH₂; DT-3, H-Arg-Gln-Ile-Lys-Ile-Trp-Phe-Gln-Asn-Arg-Arg-Met-Lys-Trp-Lys-Lys-Leu-Arg-Lys-Lys-Lys-Lys-Lys-His-OH; NVP-AAM077, [(*R*)-[(*S*)-1-(4-bromo-phenyl)-ethylamino]-(2,3-dioxo-1,2,3,4-tetrahydroquinoxalin-5-yl)-methyl]-phosphonic acid; siRNA, small interfering RNA; shRNA, short-hairpin RNA; RISC, RNA-Induced Silencing Complex; CNS, central nervous system; i.t., intrathecal.

e) Recommended Section assignment: Behavioral Pharmacology

Abstract

The present study characterizes the involvement of the *N*-methyl-D-aspartic acid receptors (NMDARs) in mediating thermal hyperalgesia induced by activation of group I metabotropic glutamate receptors (mGluRs). Intrathecal (i.t.) administration of the mGluR1/5 agonist (*S*)-3,5-DHPG to mice resulted in significant hyperalgesia as assessed by the tail immersion test. The pre-treatment of mice i.t. with CGS 19755 (selective antagonist of the NMDAR); CGP 78608 (selective antagonist at the glycine-binding site of the NMDAR); ifenprodil and Ro 25-6981 (selective antagonists of the NR2B subunit of the NMDAR); bisindolylmaleimide I and Go-7874 (inhibitors of protein kinase C) or PKI-(14-22)-amide (inhibitor of protein kinase A, dose-dependently inhibited the hyperalgesia induced by i.t. administration of the mGluR1/5 receptor agonist (*S*)-3,5-DHPG. Conversely, i.t. pre-treatment of mice with NVP-AAM077 (selective antagonist of the NR2A subunit of the NMDAR) or DT-3 (inhibitor of protein kinase G) had no effect on (*S*)-3,5-DHPG-mediated hyperalgesia. We also show for the first time that i.t. injection of pSM2-grin2b (coding for an shRNA to the NR2B subunit of the NMDAR) resulted in a dose-dependent decrease in the NR2B protein and blockade of hyperalgesia induced by activation of the mGluR1/5 in (*S*)-3,5-DHPG- treated mice. Taken together, our results suggest the hypothesis that mGluRs are coupled to the NMDAR channels through the NR2B subunit in the spinal cord, and that this coupling involves the activation of PKC and PKA.

Introduction

Glutamate is one of the most ubiquitous neurotransmitter in the central nervous system. It activates both ionotropic and metabotropic receptors and therefore it is equally essential for fast excitatory synaptic transmission and modulation of synaptic transmission. In the spinal dorsal horn, in lamina II neurons, glutamate primarily activates the ionotropic non-*N*-methyl-D-aspartic acid (non-NMDA) type alpha-amino-3-hydroxy-5-methyl-4-isoxazolepropionic acid (AMPA) and kainate receptors (Yoshimura and Jessell, 1990) while in superficial (lamina I) and deep dorsal horn neurons both non-NMDA and NMDA receptor (NMDAR) activation occurs in control conditions (Millan, 1999). Several genes encoding NMDAR subunits have been identified. These genes fall into three categories: NMDA-R1 subunit (NR1), A–D isoforms of NMDA-R2 subunit (NR2A–D), and NMDA-R3 subunit (NR3) (Kutsuwada et al., 1992). While NMDAR stimulation enhances synaptic transmission in the dorsal horn of the spinal cord, activation of the G-protein-coupled metabotropic glutamate receptors (mGluRs) serves mainly to modulate synaptic neurotransmission (Pin and Acher 2002). Eight subtypes of mGluRs have been identified and divided in three groups on the basis of pharmacological and signal transduction mechanisms and amino acid homology. Group I mGluRs (mGluR1/5) are linked to phospholipase C and the activation of protein kinase C (PKC). Group II mGluRs (mGluR2/3) and group III mGluRs (mGluR4/6/7/8) are negatively coupled to adenylyl cyclase through Gi/Go to decrease cAMP accumulation (Conn and Pin 1997).

Interestingly, group I mGluRs have been demonstrated to interact biochemically with NMDARs *in vitro*. For example, activating mGluR1 potentiated NMDAR currents in *Xenopus oocytes* leading to an increase in intracellular Ca²⁺ and activation of PKC (Lan et al. 2001). Furthermore, in mice cortical slices, NMDA-induced depolarization was enhanced by the selective mGluR1/5 agonist (*S*)-3,5-dihydroxyphenylglycine ((*S*)-3,5-DHPG), and blocked by the selective mGluR5 antagonist 2-methyl-6-(phenylethynyl)-pyridine (MPEP) (Attucci et al. 2001). In contrast to *in vitro* studies, very few *in vivo* studies have been conducted to examine the potential coupling between group I mGluRs and NMDARs in

mediating nociception in animals. The role of group I mGluRs in nociception has been well established, but less is known about the functional interaction between those receptors and the NMDARs. Activation of group I mGluRs has been demonstrated to produce nociception in animals. Intrathecal (i.t.) administration of (*S*)-3,5-DHPG was shown to induce persistent thermal hyperalgesia and mechanical allodynia (Fisher and Coderre, 1998). In addition, carrageenan-induced thermal and mechanical hyperalgesia in rats with hindpaw inflammation were blocked by i.t. of the group I mGluRs antagonist (*S*)-4-carboxy-3-hydroxyphenylglycine ((*S*)-4C3HPG) (Young et al., 1997).

There is considerable evidence that pain associated with peripheral tissue or nerve injury involves NMDAR activation (Doubell et al., 1999). Consistent with this, NMDAR antagonists have been shown to effectively alleviate pain-related behavior in animal models as well as in clinical situations (Fisher et al., 2000; Hewitt, 2000). However, NMDARs are important for normal CNS functions, and the use of NMDAR antagonists can often be limited by serious side effects, such as memory impairment, psychotomimetic effects, ataxia, motor incoordination, hallucinations and agitation (Petrenko et al., 2003). However, newly developed NMDAR antagonists at the glycine-site, NR2B sites and weak-binding channel blockers have demonstrated an improved side effect profile in animal models of pain (Brown and Krupp, 2006). More recent studies indicate that modulating the activity of NMDARs with group I mGluRs drugs might be effective in treating chronic pain (Guo et al., 2004), thus limiting the incidence of NMDA-like side effects. The goal of this study was to utilize a model of thermal hyperalgesia to investigate the mechanisms by which group I mGluRs interact with NMDARs. The hypothesis was tested that pharmacological stimulation of group I mGluRs results in the concomitant activation of NMDA receptors.

We also evaluated, for the first time, the interaction between the mGluRs and the NR2B subunit of the NMDAR at a molecular level. Functional NR2B-containing NMDARs are formed by their co-assembly with the obligatory NR1 subunits (Masuko et al., 1999). The NR1 subunits are ubiquitously expressed in the central nervous system (CNS), whereas the NR2B protein is localized predominantly in the superficial dorsal horn of the spinal cord (Boyce et al., 1999). Therefore, another aim was to investigate the role of NR2B receptor subunit in the modulation of (*S*)-3,5-DHPG-induced thermal

hyperalgesia using a more selective experimental tool of small interfering RNA (siRNA) that involves a double-stranded short-hairpin RNA (shRNA) specifically silencing the mouse NR2B.

Methods

Animals

Male Swiss Webster mice (Harlan Laboratories, Indianapolis, IN) weighing 25-30 g were housed 6 to a cage in animal care quarters and maintained at 22 ± 2 °C on a 12-hr light-dark cycle. Food and water were available *ad libitum*. The mice were brought to a test room (22 ± 2 °C, 12-hr light-dark cycle), marked for identification and allowed 18-hr to recover from transport and handling. Protocols and procedures were approved by the Institutional Animal Care and Use Committee (IACUC) at Virginia Commonwealth University Medical Center and comply with the recommendations of the IASP (International Association for the Study of Pain).

Drugs and chemicals

The following agents were purchased from Tocris Cookson Bioscience (Ellisville, MO, USA): (*S*)-3,5-dihydroxyphenylglycine [(*S*)-3,5-DHPG; mGluR1/5 agonist], α -amino-5-carboxy-3-methyl-2-thiopheneacetic acid (3-MATIDA; mGluR1 antagonist; Moroni et al., 2002), 2-methyl-6-(phenylethynyl)pyridine hydrochloride (MPEP hydrochloride; mGluR5 antagonist), *cis*-4-[phosphomethyl]-piperidine-2-carboxylic acid (CGS 19755; selective competitive NMDAR antagonist) and [(1*S*)-1-[[[7-bromo-1,2,3,4-tetrahydro-2,3-dioxo-5-quinoxaliny]methyl]amino]ethyl]phosphonic acid (CGP 78608; selective NMDAR antagonist that acts through the glycine site). The selective NR2B subunit antagonists α -(4-Hydroxyphenyl)- β -methyl-4-benzyl-1-piperidineethanol tartrate salt (ifenprodil) and [R-(R*,S*)]- α -(4-Hydroxyphenyl)- β -methyl-4-(phenylmethyl)-1-piperidinepropanol hydrochloride (Ro 25-6981) were purchased from Sigma (St. Louis, MO, USA). The following agents were purchased from Calbiochem (San Diego, CA, USA), 2-[1-(3-dimethylaminopropyl)-1H-indol-3-yl]-3-(1H-indol-3-yl)-maleimide (bisindolylmaleimide I HCl; selective inhibitor of PKC α , β I, β II, ϵ , δ , ζ isoforms), 12-(2-

Cyanoethyl)-6,7,12,13-tetrahydro-13-methyl-5-oxo-5H-indolo(2,3-a)pyrrolo(3,4-c)-carbazole (Go-7874; selective inhibitor of PKC α , β I, β II, γ isoforms) and myristolated PKI (14–22) amide [Myr-N-Gly-Arg-Thr-Gly-Arg-Arg-Asn-Ala-Ile-NH₂; PKI-(14-22)-amide; selective PKA inhibitor] as well as H-Arg-Gln-Ile-Lys-Ile-Trp-Phe-Gln-Asn-Arg-Arg-Met-Lys-Trp-Lys-Lys-Leu-Arg-Lys-Lys-Lys-Lys-Lys-His-OH (DT-3; selective PKG inhibitor). [(R)-[(S)-1-(4-bromo-phenyl)-ethylamino]-(2,3-dioxo-1,2,3,4-tetrahydroquinoxalin-5-yl)-methyl]-phosphonic acid (NVP-AAM077; selective NR2A subunit antagonist) was a generous gift from Novartis Pharma (Basel, Switzerland). The drugs were dissolved in saline or mixture of 10% dimethyl sulfoxide (Sigma, St. Louis, MO, USA), 20% Cremophor EL (Sigma, St. Louis, MO, USA), 70% saline. The appropriate drug vehicle was used as a control.

NR2B shRNA

The vector directing the transcription of a short-hairpin RNA (shRNA) specifically targeting the NR2B (*grin2b*) subunit of the mouse NMDAR as well as a shRNA Non-silencing (NS) control vector were purchased from Open Biosystems (Huntsville, AL, USA) as glycerol stocks of transformed *E. coli*. The base vector for both plasmids is a retroviral pShag Magic version 2 (pSM2). The pSM2-*grin2b* is designed for high level expression of shRNA for the mouse NR2B subunit under the control of the mouse U6 promoter. The pSM2-NS represents a negative control shRNA vector. *E. coli* were grown according to the manufacturer's recommended protocols. The plasmids were gradient-purified using cesium chloride (CsCl). The sequence of the shRNA insert in pSM2-*grin2b* was confirmed using a primer developed for the U6 promoter region (5' TGT GGA AAG GAC GAA ACA CC 3'). Sequence analysis was performed using an Applied Biosystems 377 Prism XL automated DNA sequencer by the Massey Cancer Center Nucleic Acid Synthesis and Analysis Core Resource (Virginia Commonwealth University, Richmond, VA, USA).

Arrest-In™, a polymeric transfection reagent (Open Biosystems; Huntsville, AL, USA), was used for the highly efficient delivery of both pSM2-*grin2b* and pSM2-NS plasmids into neurons. Once in the

cells Arrest-In™ promotes the entry of the shRNA containing plasmid into the nucleus where it is transcribed into a hairpin, enters the cytoplasm, and is processed by the endogenous RNAi machinery into functional siRNAs.

Intrathecal injections

Intrathecal (i.t.) injections were made through the intervertebral space in unanaesthetized mice between the L5-L6 of the spinal cord, as described by Hylden and Wilcox (1980). Briefly, a volume of 5 μ l was administered i.t. with a 28 gauge, 1/2-inch stainless steel needle connected to a 50 μ l Hamilton microsyringe, the animal being lightly restrained to maintain the position of the needle. Puncture of the dura was indicated behaviorally by a slight flick of the tail.

The tail immersion test

The warm-water tail immersion test was performed according to Coderre and Rollman (1983). The mouse was gently wrapped in a towel, held at a 45° angle to a thermostatically controlled water bath set at 50 ± 1 °C. The latency between submersion of the tail and its removal from the water by the animal was recorded, with a maximum cut-off time of 10 s to avoid tissue damage. Pre-treatment latencies were determined in mice, 3 times with an interval of 24 h starting 3 days before drug administration, in order to obtain a stable pre-drug response (basal latency). Mice with a latency value between 5.0 and 7.0 s were used. The average basal latency for the experiments was 5.7 ± 0.01 sec. The test latency after drug administration was assessed at the appropriate time. The tail immersion response was expressed as percent (%) of basal latency.

Immunoblotting

To examine changes in expression of NR2B protein in the spinal cord, seven groups of mice (n=6) were used for immunoblot analysis: naive, three pSM2-NS-treated groups (0.5, 1.0 and 1.5 $\mu\text{g}/\text{mouse}$) and three pSM2-grin2b-treated groups (0.5, 1.0 and 1.5 $\mu\text{g}/\text{mouse}$). Animals were killed by decapitation under anesthesia (pentobarbital 120 mg/kg, i.p.). Spinal cords were extracted by injecting normal saline under pressure through a 16-gauge needle into the upper sacral spine, thus forcing the spinal cord out rostrally. The L4–L6 dorsal spinal cord segments were rapidly dissected and homogenized with a hand-held pellet pestle in 250 μl lysis buffer (20 mM Tris, pH 7.5, 150 mM NaCl, 1% Nonidet P-40, 0.5% Sodium Deoxycholate, 1 mM EDTA, 0.1% SDS, Complete Protease Inhibitor Cocktail from Roche (Indianapolis, IN, USA; 1 tablet/50 ml of lysis buffer) and centrifuged at 13,000 \times g for 3 min at 25 °C. The supernatant was decanted and used for the subsequent Western blot analyses. The protein concentration of the supernatant was measured using a Pierce bicinchoninic acid (BCA) Protein Assay Kit (Pierce; Norcross, GA, USA). NR2B protein levels were determined using an immunoblotting procedure essentially as described previously (Ritter et al., 1999; Guillemette et al., 2000). Proteins were separated on a 7.5% SDS-polyacrylamide gel (Bio-Rad; Hercules, CA, USA), and transferred to a nitrocellulose membranes (Bio-Rad; Hercules, CA, USA). Membranes were blocked with SuperBlock T-20 (TBS) Blocking Buffer (Pierce; Norcross, GA, USA) and incubated overnight at 4 °C with rabbit polyclonal antibody to NR2B (1:500 dilution; Novus Biologicals; Littleton, CO, USA). Proteins were visualized by incubation with ECL Plus Western Blotting Detection Reagents (GE Healthcare; Piscataway, NJ, USA) and scanned at 200 μm resolution using the Molecular Dynamics STORM system (GE Healthcare; Piscataway, NJ, USA). Images were analyzed by using ImageQuant software 5.2 (Molecular Dynamics) and data were expressed as volume of pixilation. Because of the molecular weight disparity between NR2B and β -actin, duplicate blots were prepared at the same time and probed with a

purified mouse monoclonal anti- β -actin, peroxidase (1:35,000 dilution; Sigma, St. Louis, MO, USA) and visualized as described above and used as a loading control.

Pharmacological treatments

In the first experiment a dose response curve for (*S*)-3,5-DHPG (1.5 – 15 nmol/mouse) was performed at 10 min intervals until 80 min after the drug administration. The following experiments, then examined whether the hyperalgesic effects of (*S*)-3,5-DHPG could be inhibited by pre-treatment with various antagonists. MPEP (12.5 - 50 nmol/mouse), 3-MATIDA (0.5 - 5 nmol/mouse), CGS 19755 (0.01 - 5 pmol/mouse), CGP 78608 (1 - 100 pmol/mouse), ifenprodil (0.5 - 2 nmol/mouse), Ro 25-6981 (0.02 - 2 nmol/mouse), NVP-AAM077 (0.005 - 10 nmol/mouse), bisindolylmaleimide I (1 - 100 pmol/mouse), Go-7874 (0.25 - 2.5 nmol/mouse), PKI-(14-22)-amide (0.025 – 2.5 nmol/mouse) or DT-3 (0.01 - 10 nmol/mouse) were administered 5 min prior to a 15 nmol/mouse i.t. injection of (*S*)-3,5-DHPG (the dose that produced maximum hyperalgesia) and then re-assessed for the tail immersion test 30 min later (time point that showed maximum hyperalgesia).

In another series of experiments, mice were administered Arrest-In™ vehicle, pSM2-NS (0.5, 1.0 and 1.5 μ g/mouse) or pSM2-grin2b (0.5, 1.0 and 1.5 μ g/mouse), 7 days prior to a 15 nmol/mouse i.t. injection of (*S*)-3,5-DHPG and then re-assessed for the tail immersion test 30 min later. Spinal cords were then extracted for Western blot analyses.

Groups of 6-12 mice per dose per treatment were tested for each compound following baseline determination (discussed in the section entitled “the tail immersion test”).

Statistical analysis

Data are expressed as mean values \pm S.E.M. Time-course studies were analyzed using Two-Factor (drug treatment X time) Repeated Measures Analysis of Variance (ANOVA). A significant F-value led to *post hoc* analysis of data using the Student Newman-Keuls test with Instat 3.0 software (GraphPad

Software, San Diego, CA, U.S.A.). The influence of increasing doses of antagonists and inhibitors to block (*S*)-3,5-DHPG-induced hyperalgesia was compared to mice treated with vehicle + (*S*)-3,5-DHPG using ANOVA. Dose-dependent antagonism of (*S*)-3,5-DHPG-induced hyperalgesia led to calculation of Inhibitory Dose-50 (ID_{50}) values, using least-squares linear regression analysis followed by calculation of 95% confidence limits (95% C.L.) by the method of Bliss (Bliss, 1967).

Results

(S)-3,5-DHPG-induced hyperalgesia

I.t. administration of the mGluR1/5 agonist (*S*)-3,5-DHPG (1.5, 4.5, 7.5 and 15 nmol/mouse) induced a dose and time dependent decrease in the tail immersion reaction time [F(32,200)= 5.33; $P < 0.001$] (Fig. 1). (*S*)-3,5-DHPG at 1.5 nmol/mouse did not produce any significant hyperalgesia over the time period tested. The 4.5 nmol/mouse dose produced a 15-20% decrease in the tail immersion reaction time between 10 and 50 min following administration of (*S*)-3,5-DHPG ($P < 0.001$). The dose of 7.5 nmol/mouse produced a 25-30% decrease in the tail immersion reaction time between 10-50 min post- (*S*)-3,5-DHPG injection ($P < 0.001$). The maximum hyperalgesia was observed with the 15 nmol/mouse dose at 30-40 min ($\cong 50\%$ decrease in the tail immersion reaction time) ($P < 0.001$). All hyperalgesic effects disappeared between 70-80 min from the injection time of (*S*)-3,5-DHPG.

mGluR1/5 antagonists inhibit (*S*)-3,5-DHPG-mediated hyperalgesia

The mGluR5 antagonist MPEP, injected i.t. 5 min prior to (*S*)-3,5-DHPG, blocked in a dose-dependent manner the (*S*)-3,5-DHPG-mediated hyperalgesia [F(3,20)= 23.8; $P < 0.001$] (Table 1; Fig. 2). Post-hoc analyses indicated that the 12.5, 25 and 50 nmol/mouse of MPEP producing a 25, 55 and 85% inhibition of (*S*)-3,5-DHPG-induced hyperalgesia, respectively, were all significant ($P < 0.001$). Similarly, the mGluR1 antagonist 3-MATIDA, administered i.t. 5 min prior to (*S*)-3,5-DHPG, resulted in a dose-dependent inhibition of the (*S*)-3,5-DHPG-induced hyperalgesia [F(3,20)= 27.7; $P < 0.001$] (Table 1; Fig. 2). Post-hoc analyses indicated that the 0.5, 1 and 5 nmol/mouse of 3-MATIDA producing a 51, 67 and 98% inhibition of (*S*)-3,5-DHPG-induced hyperalgesia, respectively, were

all significant ($P < 0.001$). The two antagonists did not change the tail immersion response in control mice within the range of doses used (data not shown).

NMDAR antagonists inhibit (*S*)-3,5-DHPG-mediated hyperalgesia

Experiments were conducted to test the hypothesis that activation of group I mGluRs leads to stimulation of NMDARs. The (*S*)-3,5-DHPG-induced hyperalgesia was blocked in a dose-dependent fashion when mice were pre-treated with the competitive NMDA receptor antagonist CGS 19755 [F(3,20)=63.4; $P < 0.001$] (Table 1; Fig 3). Post-hoc analyses indicated that the 0.01, 1 and 5 pmol/mouse doses of CGS 19755 producing a 32, 53, and 91% inhibition of (*S*)-3,5-DHPG-induced hyperalgesia, respectively, were all significant ($P < 0.001$). In addition, the NMDA glycine site antagonist CGP 78608, administered i.t. 5 min prior to (*S*)-3,5-DHPG, induced a dose-dependent inhibition of the (*S*)-3,5-DHPG-induced hyperalgesia [F(3,49)= 65.5; $P < 0.001$] (Table 1; Fig 3). Post-hoc analyses indicated that the 1, 10 and 100 pmol/mouse doses of CGP 78608 producing a 19, 57 and 94% inhibition of (*S*)-3,5-DHPG-induced hyperalgesia, respectively, were all significant ($P < 0.001$).

In a similar fashion, pre-treatment with the selective NR2B subunit antagonists ifenprodil and Ro 25-6981 but not the selective NR2A subunit antagonist NVP-AAM077, blocked the effects of (*S*)-3,5-DHPG. Ifenprodil dose-dependently inhibited the the (*S*)-3,5-DHPG-induced hyperalgesia [F(3,50)= 97.2; $P < 0.001$] (Table 1; Fig 3). Post-hoc analyses indicated that the 0.5, 1 and 2 nmol/mouse of ifenprodil producing 19, 61 and 94% inhibition (*S*)-3,5-DHPG-induced hyperalgesia, respectively, were all significant ($P < 0.001$). Ro 25-6981 also resulted in a dose-dependent inhibition of the (*S*)-3,5-DHPG-induced hyperalgesia [F(3,61)= 82.7; $P < 0.001$] (Table 1; Fig 3). Post-hoc analyses indicated that the 25 and 50 nmol/mouse of Ro 25-6981 producing a 21 and 99% inhibition of (*S*)-3,5-DHPG-induced hyperalgesia, respectively, were significant ($P < 0.001$), whereas the dose of 12.5 nmol/mouse had no significant effect on the (*S*)-3,5-DHPG-induced hyperalgesia.

All the doses of the drugs that blocked (*S*)-3,5-DHPG-induced hyperalgesia were inactive when administered alone to mice (data not shown). Very high doses of NVP-AAM077 (5 - 10 nmol/mouse) impaired motor activity in control mice and produced a maximum response in the tail-immersion test (data not shown). The highest inactive dose of NVP-AAM077 (0.5 nmol/mouse), that did not elicit toxic effects in control mice, was tested and it had no effect on the (*S*)-3,5-DHPG-induced hyperalgesia (Fig. 3).

Signal transduction between type I mGluRs and NMDARs activation

The hyperalgesia observed in (*S*)-3,5-DHPG-treated mice was blocked by pre-treatment with the selective inhibitor of PKC α , β I, β II, ϵ , δ , ζ , bisindolylmaleimide I, the selective inhibitor of PKC α , β I, β II, γ , Go-7874 or the selective PKA inhibitor, PKI-(14-22)-amide (Table 1; Fig. 4). Bisindolylmaleimide I, injected i.t. 5 min prior to (*S*)-3,5-DHPG, blocked in a dose-dependent manner the (*S*)-3,5-DHPG-induced hyperalgesia [F(3,44)= 61.4; $P < 0.001$]. Post-hoc analyses indicated that the 0.1, 10 and 100 pmol/mouse of bisindolylmaleimide I producing a 27, 56 and 89% inhibition of (*S*)-3,5-DHPG-induced hyperalgesia, respectively, were all significant ($P < 0.001$). In a similar fashion, Go-7874 dose-dependently inhibited the (*S*)-3,5-DHPG-mediated hyperalgesia [F(3,47)= 78.7; $P < 0.001$] (Table 1; Fig. 4). Post-hoc analyses indicated that the 0.5, 1 and 2.5 nmol/mouse of Go-7874 producing a 20, 60 and 100% inhibition of (*S*)-3,5-DHPG-induced hyperalgesia, respectively, were all significant ($P < 0.001$).

On the other hand, the selective PKA inhibitor PKI-(14-22)-amide was also shown to block the (*S*)-3,5-DHPG-mediated hyperalgesia in a dose-dependent manner [F(3,38)= 70.4; $P < 0.001$] (Table 1; Fig. 4). Post-hoc analyses indicated that the 0.25 and 2.5 nmol/mouse of PKI-(14-22)-amide producing a 58 and 91% inhibition of (*S*)-3,5-DHPG-induced hyperalgesia, respectively, were significant ($P < 0.001$). Conversely, the dose of 0.025 nmol/mouse of PKI-(14-22)-amide did not produce any significant

effect in inhibiting the (*S*)-3,5-DHPG-induced hyperalgesia. It is worth mentioning that the selective PKG inhibitor, DT-3 had no effect on hyperalgesia (Fig. 4).

All the doses of the PKC and PKA inhibitors that blocked (*S*)-3,5-DHPG-induced hyperalgesia were inactive when administered alone to mice (data not shown). High doses of DT-3 (0.01 - 10 nmol/mouse) induced motor deficits in control mice and produced a maximum response in the tail-immersion test. However, the highest inactive dose of DT-3 (2 nmol/mouse) failed to block (*S*)-3,5-DHPG-induced hyperalgesia (Fig. 4).

pSM2-grin2b injection silences the NR2B gene and blocks the (*S*)-3,5-DHPG-mediated hyperalgesia

Mice were injected i.t. with 1.5 μ g of either pSM2-grin2b, an NR2B shRNA expression plasmid, or pSM2-NS, a non-silencing shRNA. As seen in Figure 5, the 7 days later (*S*)-3,5-DHPG-induced hyperalgesia was blocked by the pSM2-grin2b expression plasmid, but not by the pSM2-NS control vector treatment ($F(3,20) = 29.3$; $P < 0.001$). The blockade of hyperalgesia was correlated with diminished protein levels of the NR2B subunit of the NMDAR shown in Western blotting. Mice injected with pSM2-grin2b showed a dose-dependent decrease in NR2B subunit protein levels [$F(3,20) = 30.4$; $P < 0.001$] (Fig. 6). Post-hoc analyses indicated that the 0.5, 1 and 1.5 μ g/mouse of pSM2-grin2b producing a 30, 41 and 53% decreases in the relative NR2B protein levels as % of control, respectively, were all significant ($P < 0.001$). The (*S*)-3,5-DHPG-induced hyperalgesia was unaffected by the transfecting agent, Arrest-In™. It is worth mentioning that the non-silencing shRNA had no effect on the tail immersion reaction time in tested mice.

Discussion

The present study addresses the coupling of the group I mGluRs to the NMDARs in mediating thermal hyperalgesia in mice. We showed that competitive NMDAR antagonists and glycine site NMDAR antagonists blocked (*S*)-3,5-DHPG-induced hyperalgesia. The link between mGluR and NMDAR receptors was further strengthened by our data demonstrating, for the first time, that gene knockdown of the NR2B subunit of the NMDAR blocked the hyperalgesia as well. In addition, the study addressed signal pathways involving group I mGluR-mediated PKC and PKA activation of the NMDAR to express hyperalgesia in mice. These findings suggest that mGluR activation is key to initiating enhanced NMDA receptor responses. Thus, the ionotropic function of the NMDARs in mediating thermal hyperalgesia *in vivo* is subject to regulation that is initiated by mGluRs/G-protein-linked mechanisms.

Antagonism of type I mGluRs and NMDARs blocks the (S)-3,5-DHPG-induced hyperalgesia

It is known that activation of group I mGluRs produces nocifensive behaviors in rats (Lorrain et al., 2002), although the mechanisms of these effects were unclear. A number of studies have indicated a role for group I mGluRs in central sensitization and hyperalgesia (Fisher andCoderre, 1996; Neugebauer et al., 1999; Karim et al., 2001). Conversely, i.t. application of group II and group III agonists did not produce nociceptive effects (Fisher and Coderre, 1996); moreover, in a rat model of neuropathic pain, they were shown to decrease mechanical and cold allodynia (Fisher et al., 2002). Evidence thus far has suggested that group I mGluRs tend to be excitatory, while groups II and III mGluRs have an inhibitory role in the spinal cord dorsal horn. In the present study, i.t. administration of the mGluR1/5 agonist (*S*)-3,5-DHPG to mice resulted in significant hyperalgesia as assessed by the tail immersion test. The pre-treatment of mice with mGluR1 or mGluR5 antagonists dose-dependently blocked the development of thermal hyperalgesia in mice. These antagonists given i.t. did not produce an effect in control mice, suggesting a selective effect on (*S*)-3,5-DHPG-induced hyperalgesia. Importantly, competitive antagonists of the NMDAR or its glycine-binding site significantly blocked group I mGluR-mediated hyperalgesia,

suggesting that the coupling between mGluR-NMDAR facilitates ionotropic synaptic transmission and spinal desensitization.

NR2B gene knockdown blocks the (S)-3,5-DHPG-induced hyperalgesia

The present study addresses the coupling of the group I mGluRs to the NMDARs in mediating thermal hyperalgesia in mice. Competitive antagonism of the NMDAR or its glycine-binding site significantly blocked group I mGluR-mediated hyperalgesia. We also showed for the first time that gene knockdown of the NR2B subunit of the NMDAR or pre-treatment with a selective NR2B subunit antagonist blocks (S)-3,5-DHPG-induced hyperalgesia. These findings suggest that the coupling between mGluR-NMDAR facilitates ionotropic synaptic transmission and spinal sensitization. Our results indicate that NR2B subunits in the spinal cord play an important role in maintaining functional NMDARs. In contrast, recent evidence indicates that nociceptive stimuli were more selective at increasing NR2A subunit phosphorylation in the brain rather than in the spinal cord. In a model of inflammation, tyrosine-phosphorylation of NR2A was up-regulated in the rostral ventromedial medulla (Turnbach et al., 2003), while it was unchanged at the spinal level (Guo et al., 2002). This could account for why the NR2A subunit antagonist NVP-AAM077 failed to significantly block (S)-3,5-DHPG-induced hyperalgesia (Fig. 3). These findings suggest that the activation of mGluRs is key to initiating enhanced NMDA receptor responses.

Signal transductions mechanisms linking the type I mGluRs and the NMDARs

The (S)-3,5-DHPG-induced hyperalgesia was blocked by PKC, PKA but not PKG inhibitors, indicating that activation of mGluR receptors leads to increases in the activity of both PKC and PKA. mGluR1/5 receptors stimulate phospholipase C β through G $_{q/11}$ proteins to convert PIP $_2$ into diacylglycerol and IP $_3$. Diacylglycerol activates Ca $^{2+}$ -dependent (conventional) and independent (novel) PKC isoforms, which can phosphorylate serine/threonine sites on the NMDAR (Sanchez-Perez and Felipe, 2005). Stimulation of mGluR receptors in rats with neuropathic pain leads to NMDAR-induced sensitization and

increases in PKC activity. This effect was prevented by transient knockdown of mGluR1 receptors with antisense (Fundytus et al., 2001). In addition, mGluRs stimulation could increase the activity of PKA through homer protein-linked stimulation of IP₃ receptors (Sala et al., 2005). The Ca²⁺ that is released from IP₃-sensitive Ca²⁺ pools is known to stimulate the Ca⁺⁺-dependent isoforms of adenylyl cyclase. The finding that a selective PKG inhibitor could not block the (S)-3,5-DHPG-induced hyperalgesia confirms the lack of linkage between mGluRs stimulation and activation of the guanylyl cyclase pathway. Taken together, it could be suggested that the ionotropic function of the NMDARs in mediating thermal hyperalgesia *in vivo* is subject to regulation that is initiated by mGluRs/G-protein-linked mechanisms.

Protein structure linking mGluRs to NMDARs

The spinal dorsal horn is the major site for initial nociceptive processing. The results of our study confirm previous co-immunoprecipitation experiments which suggested in the dorsal horn, that the mGluR-Homer-Shank complex and NMDAR are biochemically linked through related postsynaptic density proteins (PSD) such as PSD-95 and Shank (Guo et al., 2004). The cytoskeletal elements and adaptor proteins that make up the post-synaptic complex linking the mGluR to the NMDAR also include protein kinases (Tezuka et al., 1999; Lei et al., 2002; Guo et al., 2004) that are important modulators of NMDAR channels. Accordingly, we suggest that the NR2B subunit is phosphorylated by kinases intrinsic to this protein complex. The present study shows that the effects of group I mGluR agonists are coupled to NR2B phosphorylation and that this coupling requires PKC, PKA but not PKG activation. The coupling of the mGluRs to the NMDARs in dorsal horn neurons is supported by the fact that selective mGluR antagonists block inflammation-induced NR2B tyrosine-phosphorylation and selective mGluR agonist-induced NR2B tyrosine-phosphorylation in spinal slices (Guo et al., 2004). Previous studies have shown that activation of group I mGluRs enhances NMDA-induced currents (Bond and Lodge, 1995) and the NMDA-mediated increase in intracellular calcium concentration in dorsal horn neurons (Bleakman et al., 1992). A role of the mGluRs in central sensitization and persistent pain has been suggested previously (Morisset and Nagy, 1996; Neugebauer et al., 1999; Karim et al., 2001). In addition, it has been found that

a co-activation of hippocampal mGluRs and NMDARs is required for the induction of long-term potentiation (LTP) (Fujii et al. 2004). Moreover, in mice lacking mGluR5, LTP was significantly reduced in NMDAR-dependent pathways like the CA1 region and dentate gyrus of the hippocampus. However, LTP was not altered in the CA3 region, an NMDAR-independent pathway (Lu et al. 1997).

NMDAR-NR2B subunit provides a new target for pain management

In summary, our results demonstrate a coupling between the mGluR and the NR2B subunit of the NMDAR in the spinal cord, and this coupling involves the activation of PKC and PKA mechanisms. Ongoing projects in our laboratory are targeting the structural proteins that link mGluRs and NMDARs and their role in pain transmission in acute and chronic animal pain models. These biochemical events are correlated with the development of thermal hyperalgesia and may underlie the mechanisms of spinal sensitization. An important implication from the present study is that mGluRs facilitate ionotropic synaptic transmission as a mechanism of modulation in the spinal cord. It is known that phosphorylation of the NMDAR results in an increase in NMDAR channel current and Ca^{2+} influx through the channel (Wang and Salter, 1994). Thus, one functional consequence of mGluR activation under painful stimuli is to prime NMDAR for further enhanced hyperexcitability. This mechanism may be a critical initiator for central nociceptive sensitization.

Acknowledgments

We thank Joshua A. Seager for valuable technical assistance during these studies.

References

Attucci S, Carla V, Mannaioni G and Moroni F (2001) Activation of type 5 metabotropic glutamate receptors enhances NMDA responses in mice cortical wedges. *Br J Pharmacol* **132**: 799-806.

Bleakman D, Rusin KI, Chard PS, Glaum SR and Miller RJ (1992) Metabotropic glutamate receptors potentiate ionotropic glutamate responses in the rat dorsal horn. *Mol Pharmacol* **42**: 192-196.

Bliss CI. (1967) *Statistics in Biology* p 439, McGraw-Hill, New York.

Bond A and Lodge D (1995) Pharmacology of metabotropic glutamate receptor-mediated enhancement of responses to excitatory and inhibitory amino acids on rat spinal neurones in vivo. *Neuropharmacology* **34**: 1015-1023.

Boyce S, Wyatt A, Webb JK, O'Donnell R, Mason G, Rigby M, Sirinathsinghji D, Hill RG and Rupniak NM (1999) Selective NMDA NR2B antagonists induce antinociception without motor dysfunction: correlation with restricted localisation of NR2B subunit in dorsal horn. *Neuropharmacology* **38**: 611-623.

Coderre TJ and Rollman GB (1983) Naloxone hyperalgesia and stress-induced analgesia in rats. *Life Sci* **32**: 2139-246.

Conn PJ and Pin JP (1997) Pharmacology and functions of metabotropic glutamate receptors. *Annu Rev Pharmacol Toxicol* **37**: 205-237.

Doubell TP, Mannion RJ and Woolf CJ (1999) The dorsal horn: state-dependent sensory processing, plasticity and the generation of pain, in *Textbook of pain* (Wall PD and Melzack R, eds) pp 165-181, Churchill Livingstone, London.

Fisher K andCoderre TJ (1996) The contribution of metabotropic glutamate receptors (mGluRs) to formalin-induced nociception. *Pain* **68**: 255-263.

Fisher K and Coderre TJ (1998) Hyperalgesia and allodynia induced by intrathecal (RS)-dihydroxyphenylglycine in rats. *Neuroreport* **9**: 1169-1172.

Fisher K, Coderre TJ and Hagen NA (2000) Targeting the N-methyl-D-aspartate receptor for chronic pain management. Preclinical animal studies, recent clinical experience and future research directions. *J Pain Symptom Manage* **20**: 358-373.

Fisher K, Lefebvre C and Coderre TJ (2002) Antinociceptive effects following intrathecal pretreatment with selective metabotropic glutamate receptor compounds in a rat model of neuropathic pain. *Pharmacol Biochem Behav* **73**: 411-418.

Fujii S, Sasaki H, Mikoshiba K, Kuroda Y, Yamazaki Y, Mostafa Taufiq A and Kato H (2004) A chemical LTP induced by co-activation of metabotropic and N-methyl-D-aspartate glutamate receptors in hippocampal CA1 neurons. *Brain Res* **999**: 20-28.

Fundyus ME, Yashpal K, Chabot JG, Osborne MG, Lefebvre CD, Dray A, Henry JL and Coderre TJ (2001) Knockdown of spinal metabotropic glutamate receptor 1 (mGluR(1)) alleviates pain and restores opioid efficacy after nerve injury in rats. *Br J Pharmacol* **132**: 354-367.

Gschwendt M, Furstenberger G, Leibersperger H, Kittstein W, Lindner D, Rudolph C, Barth H, Kleinschroth J, Marme D and Schachtele C (1995) Lack of an effect of novel inhibitors with high specificity for protein kinase C on the action of the phorbol ester 12-O-tetradecanoylphorbol-13-acetate on mouse skin in vivo. *Carcinogenesis* **16**: 107-111.

Guillemette C, Ritter JK, Auyeung DJ, Kessler FK and Housman DE (2000) Structural heterogeneity at the UDP-glucuronosyltransferase 1 locus: functional consequences of three novel missense mutations in the human UGT1A7 gene. *Pharmacogenetics* **10**: 629-644.

Guo W, Zou S, Guan Y, Ikeda T, Tal M, Dubner R and Ren K (2002a) Tyrosine phosphorylation of the NR2B subunit of the NMDA receptor in the spinal cord during the development and maintenance of inflammatory hyperalgesia. *J Neurosci* **22**: 6208-6217.

Guo W, Wei F, Zou S, Robbins MT, Sugiyo S, Ikeda T, Tu JC, Worley PF, Dubner R and Ren K (2004) Group I metabotropic glutamate receptor NMDA receptor coupling and signaling cascade mediate spinal dorsal horn NMDA receptor 2B tyrosine phosphorylation associated with inflammatory hyperalgesia. *J Neurosci* **24**: 9161-9173.

Hewitt DJ (2000) The use of NMDA-receptor antagonists in the treatment of chronic pain. *Clin J Pain* **16(2 Suppl)**: S73-S79

Hylden JL and Wilcox GL (1980) Intrathecal morphine in mice: a new technique. *Eur J Pharmacol* **67**: 313-316.

Karim F, Wang CC and Gereau IV RW (2001) Metabotropic glutamate receptor subtypes 1 and 5 are activators of extracellular signal-regulated kinase signaling required for inflammatory pain in mice. *J Neurosci* **21**: 3771-3779.

Kutsuwada T, Kashiwabuchi N, Mori H, Sakimura K, Kushiya E, Araki K, Meguro H, Masaki H, Kumanishi T, Arakawa M and Mishina M (1992) Molecular diversity of the NMDA receptor channel. *Nature* **358**: 36-41.

Lan JY, Skeberdis VA, Jover T, Zheng X, Bennett MV and Zukin RS (2001) Activation of metabotropic glutamate receptor 1 accelerates NMDA receptor trafficking. *J Neurosci* **21**: 6058-6068.

Lei G, Xue S, Chery N, Liu Q, Xu J, Kwan CL, Fu YP, Lu YM, Liu M, Harder KW and Yu XM (2002) Gain control of N-methyl-D-aspartate receptor activity by receptor-like protein tyrosine phosphatase alpha. *EMBO J* **21**: 2977-2989.

Lu YM, Jia Z, Janus C, Henderson JT, Gerlai R, Wojtowicz JM and Roder JC (1997) Mice lacking metabotropic glutamate receptor 5 show impaired learning and reduced CA1 long-term potentiation (LTP) but normal CA3 LTP. *J Neurosci* **17**: 5196-205.

Masuko T, Kashiwagi K, Kuno T, Nguyen ND, Pahk AJ, Fukuchi J, Igarashi K and Williams K (1999) A regulatory domain (R1-R2) in the amino terminus of the N-methyl-D-aspartate receptor: effects of spermine, protons, and ifenprodil, and structural similarity to bacterial leucine/isoleucine/valine binding protein. *Mol Pharmacol* **55**: 957-969.

Millan MJ (1999) The induction of pain: an integrative review. *Prog Neurobiol* **57**: 1-164.

Morisset V and Nagy F (1996) Modulation of regenerative membrane properties by stimulation of metabotropic glutamate receptors in rat deep dorsal horn neurons. *J Neurophysiol* **76**: 2794-2798.

Moroni F, Attucci S, Cozzi A, Meli E, Picca R, Scheideler MA, Pellicciari R, Noe C, Sarichelou I and Pellegrini-Giampietro DE (2002) The novel and systemically active metabotropic glutamate 1 (mGlu1) receptor antagonist 3-MATIDA reduces post-ischemic neuronal death. *Neuropharmacology* **42**: 741-751.

Neugebauer V, Chen PS and Willis WD (1999) Role of metabotropic glutamate receptor subtype mGluR1 in brief nociception and central sensitization of primate STT cells. *J Neurophysiol* **82**: 272-282.

Petrenko AB, Yamakura T, Baba H and Shimoji K (2003) The role of N-methyl-D-aspartate (NMDA) receptors in pain: a review. *Anesth Analg* **97**: 1108-1116.

Pin JP and Acher F (2002) The metabotropic glutamate receptors: structure, activation mechanism and pharmacology. *Curr Drug Targets CNS Neurol Disord* **1**: 297-317.

Ritter JK, Kessler FK, Thompson MT, Grove AD, Auyeung DJ and Fisher RA (1999) Expression and inducibility of the human bilirubin UDP-glucuronosyltransferase UGT1A1 in liver and cultured primary hepatocytes: evidence for both genetic and environmental influences. *Hepatology* **30**: 476-484.

Sala C, Roussignol G, Meldolesi J and Fagni L (2005) Key role of the postsynaptic density scaffold proteins Shank and Homer in the functional architecture of Ca²⁺ homeostasis at dendritic spines in hippocampal neurons. *J Neurosci* **25**: 4587-4592.

Sanchez-Perez AM and Felipo V (2005) Serines 890 and 896 of the NMDA receptor subunit NR1 are differentially phosphorylated by protein kinase C isoforms. *Neurochem Int* **47**: 84-91.

Tezuka T, Umemori H, Akiyama T, Nakanishi S and Yamamoto T (1999) PSD-95 promotes Fyn-mediated tyrosine phosphorylation of the N-methyl-D-aspartate receptor subunit NR2A. *Proc Natl Acad Sci USA* **96**: 435-440.

Turnbach ME, Guo W, Dubner R and Ren K (2003) Inflammation induces tyrosine phosphorylation of the NR2A subunit and serine phosphorylation of NR1 subunits in the rat rostral ventromedial medulla. *Soc Neurosci Abstr* **29**: 695.13.

Yoshimura M and Jessell T (1990) Amino acid-mediated EPSPs at primary afferent synapses with substantia gelatinosa neurones in the rat spinal cord. *J Physiol* **430**: 315-335.

Young MR, Fleetwood-Walker SM, Dickinson T, Blackburn-Munro G, Sparrow H, Birch PJ and Bountra C (1997) Behavioural and electrophysiological evidence supporting a role for group I metabotropic glutamate receptors in the mediation of nociceptive inputs to the rat spinal cord. *Brain Res* **777**: 161-169.

Wang YT and Salter MW (1994) Regulation of NMDA receptors by tyrosine kinases and phosphatases. *Nature* **369**: 233-235.

Footnotes

a) This work was supported in part by NIDA grants: DA-01647, K05-DA00480 and DA-020836.

b) Send reprints to: William L. Dewey, Virginia Commonwealth University Medical Center, Department of Pharmacology and Toxicology, Medical Sciences Building, P.O. Box 980613 , Richmond, VA 23298.

E-mail: wdewey@vcu.edu

Legends for Figures

Figure 1. (*S*)-3,5-DHPG-mediated hyperalgesia. Mice (n= 6-10) with pre-determined tail immersion baseline were injected i.t. with the mGluR1/5 agonist, (*S*)-3,5-DHPG (1.5 – 15 nmol/mouse) and re-tested for their tail immersion response every 10 min for up to 80 min. Data are expressed as mean % of basal latency \pm S.E.M.. ^a value significantly different from vehicle-injected mice and ^b value significantly different from 0 min time point.

Figure 2. Inhibition of (*S*)-3,5-DHPG-mediated hyperalgesia by mGluR antagonists. Mice (n= 7-12), with pre-determined tail immersion baseline, were injected i.t. with either the mGluR5 antagonist, MPEP or the mGluR1 antagonist, 3-MATIDA; and 5 min later administered the (*S*)-3,5-DHPG. Mice were re-assessed for their tail immersion reaction time 30 min following the (*S*)-3,5-DHPG. Data are expressed as mean % of basal latency \pm S.E.M. ***Value significantly different from vehicle-injected mice at $P<0.05$, +++Value significantly different from (*S*)-3,5-DHPG-injected mice at $P<0.05$.

Figure 3. Effects of NMDAR antagonism on (*S*)-3,5-DHPG-mediated hyperalgesia. Mice (n= 8-12), with pre-determined tail immersion baseline, were injected i.t. with the selective competitive NMDAR antagonist, CGS 19755; the selective NMDAR antagonist that acts through the glycine site, CGP 78608; the selective NR2A subunit antagonist, NVP-AAM077; or the selective NR2B subunit antagonists ifenprodil and Ro 25-6981; and 5 min later administered the (*S*)-3,5-DHPG. Mice were re-assessed for their tail immersion reaction time 30 min following the (*S*)-3,5-DHPG. Data are expressed as mean % of basal latency \pm S.E.M. ***Value significantly different from vehicle-injected mice at $P<0.05$, +++Value significantly different from (*S*)-3,5-DHPG-injected mice at $P<0.05$.

Figure 4. Effects of protein kinase inhibitors on (S)-3,5-DHPG-mediated hyperalgesia. Mice (n= 6-10), with pre-determined tail immersion baseline, were injected i.t. with the PKC inhibitors, bisindolylmaleimide I and Go-7874; the PKA inhibitor, PKI-(14-22)-amide; or the PKG inhibitor, DT-3; and 5 min later administered the (S)-3,5-DHPG. Mice were re-assessed for their tail immersion reaction time 30 min following the (S)-3,5-DHPG. Data are expressed as mean % of basal latency \pm S.E.M. ***Value significantly different from vehicle-injected mice at $P<0.05$, +++Value significantly different from (S)-3,5-DHPG-injected mice at $P<0.05$.

Figure 5. Effect of knockdown of the NR2B subunit of the NMDAR on (S)-3,5-DHPG-mediated hyperalgesia. Mice (n= 6-8), with pre-determined tail immersion baseline, were injected i.t. with either pSM2-grin2b, encoding an shRNA for the NR2B subunit of the NMDAR, or pSM2-NS, encoding a non-silencing control shRNA; and 7 days later were re-tested for their tail immersion baseline before being administered the (S)-3,5-DHPG. Mice were re-assessed for their tail immersion reaction time 30 min following the (S)-3,5-DHPG. Data are expressed as mean % of basal latency \pm S.E.M. ***Value significantly different from vehicle-injected mice at $P<0.05$, +++Value significantly different from (S)-3,5-DHPG-injected mice at $P<0.05$.

Figure 6. Decrease in NR2B subunit protein after direct *in vivo* transfection with pSM2-grin2b. **The upper panel** is a representative Western blot showing changes in the level of NR2B subunit protein observed in spinal cords of mice, 7 days after i.t. injection (1.5 μ g/mouse) of either encoding an shRNA for the NR2B subunit of the NMDAR, or pSM2-NS, encoding a non-silencing control shRNA. **The lower panel** shows the relative NR2B subunit protein level expression as a function of the pSM2-grin2b dose. Data are expressed as means \pm S.E.M.; n = 6 mice.

Table 1. Treatment dose effects for antagonism of the hyperalgesic effects of i.t. (S)-3,5-DHPG.

Pharmacological reagent (dose per mouse)	% of basal latency \pm S.E.M. Co-treatment with (S)-3,5-DHPG	ID50 value (95% C.L.)
<u>MPEP</u>		
0.0	52.87 \pm 2.32	23.90 nmol (95% C.L. 19.7 to 28.9)
12.5 nmol	56.51 \pm 5.88*	
25 nmol	81.74 \pm 2.93*	
50 nmol	96.02 \pm 3.62*	
<u>3-MATIDA</u>		
0.0	51.62 \pm 2.70	0.07 nmol (95% C.L. 0.01 to 0.5)
0.5 nmol	77.59 \pm 5.61*	
1 nmol	85.70 \pm 2.70*	
5 nmol	101.07 \pm 0.87*	
<u>CGS 19755</u>		
0.0	52.43 \pm 2.33	0.10 pmol (95% C.L. 0.06 to 0.17)
0.01 pmol	69.41 \pm 1.21*	
1 pmol	79.52 \pm 3.24*	
5 pmol	99.90 \pm 1.97*	
<u>CGP 78608</u>		
0.0	51.38 \pm 1.33	6.70 pmol (95% C.L. 4.3 to 10.6)
1 pmol	61.29 \pm 2.64*	
10 pmol	81.34 \pm 5.07*	
100 pmol	99.82 \pm 2.44*	
<u>Ifenprodil</u>		
0.0	52.87 \pm 1.12	0.78 nmol (95% C.L. 0.64 to 95)
0.5 nmol	62.53 \pm 4.15*	
1 nmol	84.54 \pm 2.51*	
2 nmol	101.32 \pm 3.28*	
<u>Ro 25-6981</u>		
0.0	51.49 \pm 0.97	0.33 nmol (95% C.L. 0.21 to 52)
12.5 nmol	47.81 \pm 4.07	
25 nmol	63.07 \pm 3.91*	
50 nmol	102.94 \pm 2.82*	
<u>Bisindolylmaleimide I</u>		
0.0	52.38 \pm 2.73	0.49 pmol (95% C.L. 0.04 to 5.60)
0.1 pmol	66.21 \pm 4.43*	
10 pmol	81.45 \pm 2.26*	
100 pmol	98.97 \pm 4.91*	

<u>Go-7874</u>	51.76 ± 3.12	0.89 nmol (95% C.L. 0.76 to 1.03)
0.0	61.04 ± 3.52*	
0.5 nmol	82.82 ± 1.08*	
1 nmol	105.82 ± 2.23*	
2.5 nmol		
<u>PKI-(14-22)-amide</u>		0.18 nmol (95% C.L. 0.11 to 0.29)
0.0	53.53 ± 1.62	
0.025 nmol	57.40 ± 4.07	
0.25 nmol	84.33 ± 3.92*	
2.5 nmol	101.86 ± 1.75*	

Mice (n= 7-12), with pre-determined tail immersion baseline, were injected i.t. with either the mGluR5 antagonist, MPEP; the mGluR1 antagonist, 3-MATIDA; the selective competitive NMDAR antagonist, CGS 19755; the selective NMDAR antagonist that acts through the glycine site, CGP 78608; the selective NR2B subunit antagonists ifenprodil and Ro 25-6981; or the PKC inhibitors, bisindolylmaleimide I and Go-7874 and the PKA inhibitor, PKI-(14-22)-amide. The (*S*)-3,5-DHPG was administered to the mice 5 min later and at 30 min from its injection, the mice were re-assessed for their tail immersion reaction time. Data are expressed as mean % of basal latency ± S.E.M. The ED50 values with 95% confidence limits were calculated for the antagonists and inhibitors co-administered with (*S*)-3,5-DHPG. *Value significantly different from mice injected with Vehicle + (*S*)-3,5-DHPG at $P < 0.05$

Figure 1

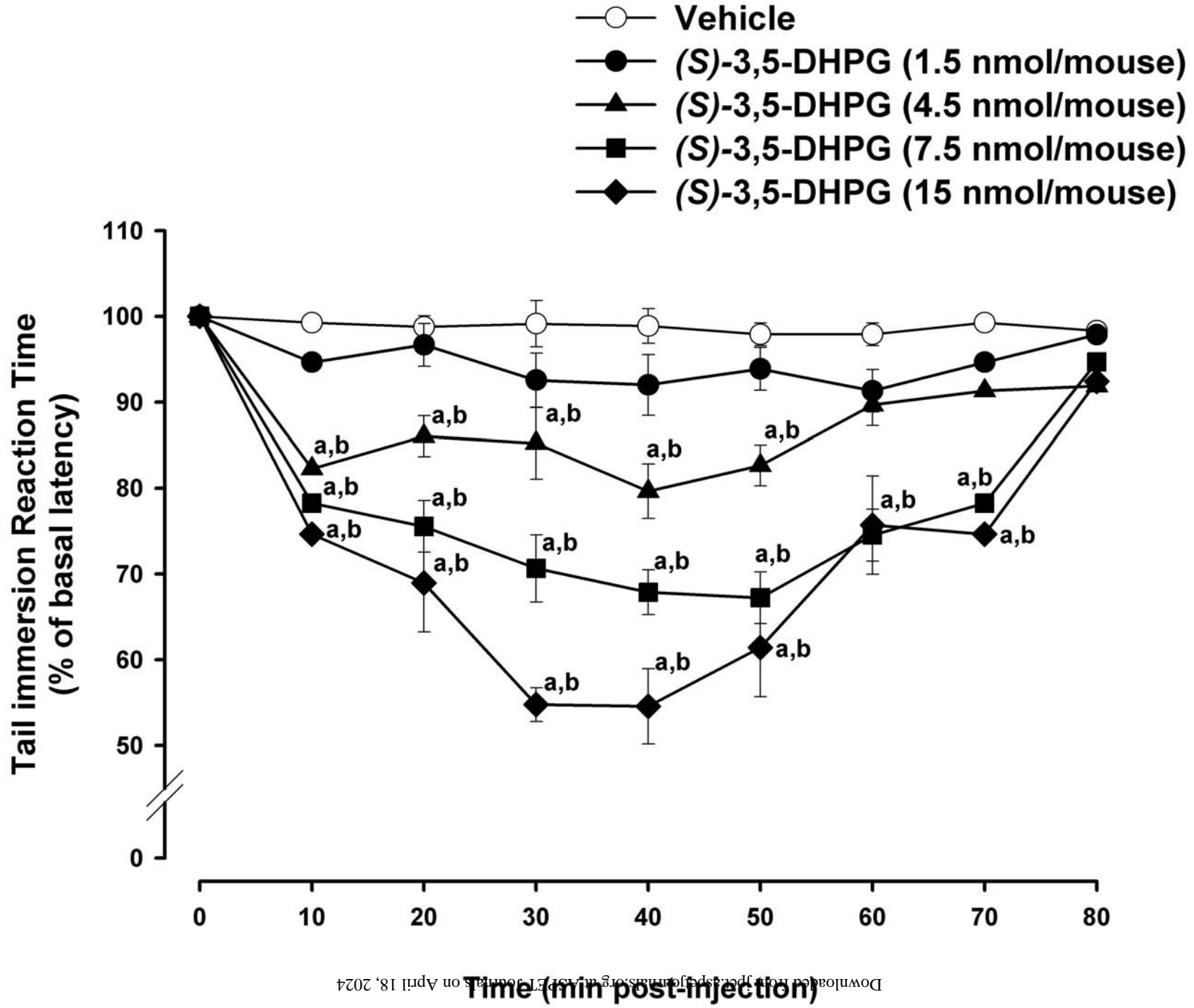
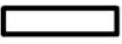





Figure 2

-  Vehicle + Vehicle
-  Vehicle + (S)-3,5-DHPG (15 nmol/mouse)
-  MPEP (50 nmol/mouse) + (S)-3,5-DHPG
-  3-MATIDA (5 nmol/mouse) + (S)-3,5-DHPG

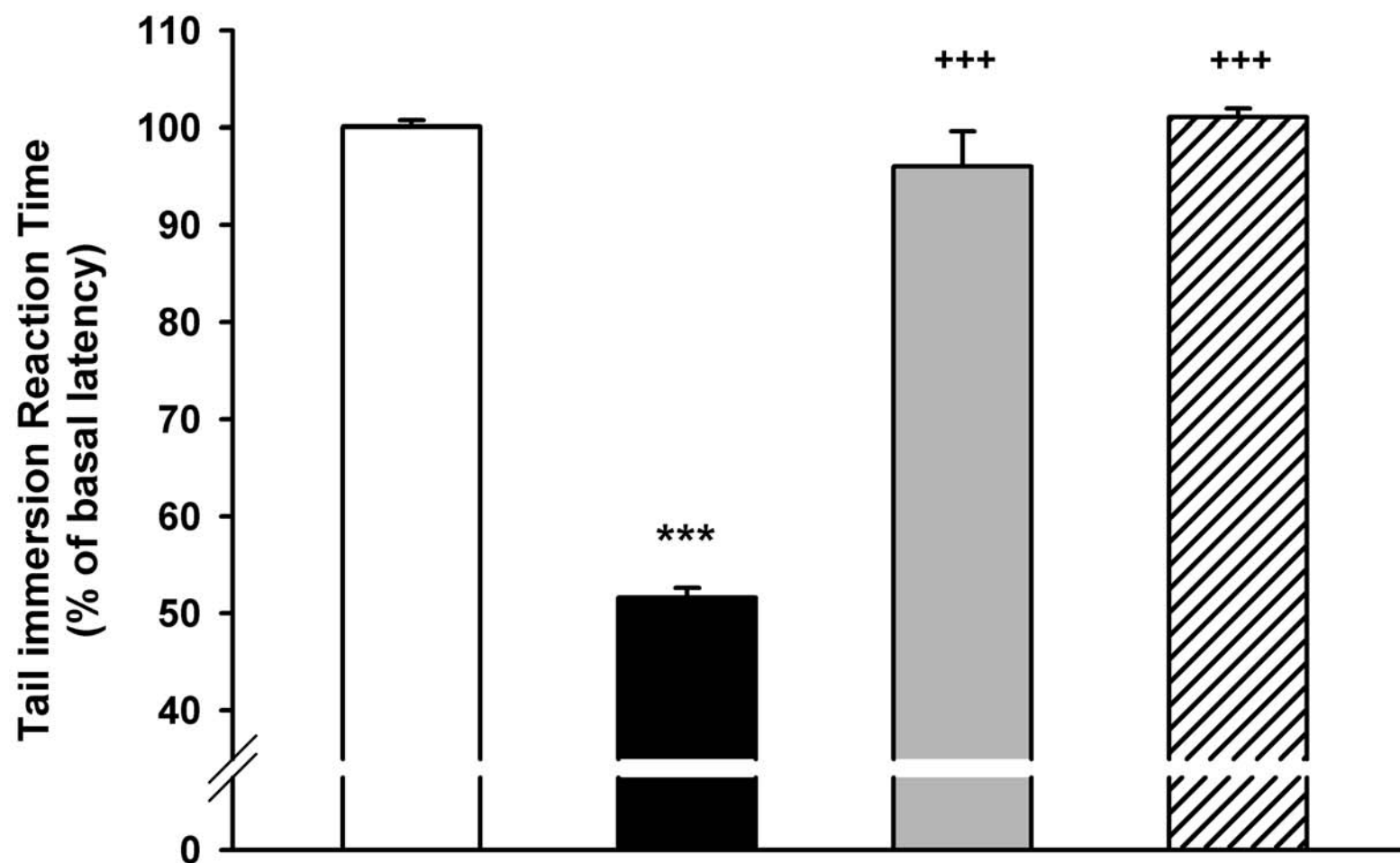









Figure 3

-  Vehicle + Vehicle
-  Vehicle + (S)-3,5-DHPG (15 nmol/mouse)
-  CGS 19755 (5 pmol/mouse) + (S)-3,5-DHPG
-  CGP 78608 (0.1 nmol/mouse) + (S)-3,5-DHPG
-  NVP-AAM077 (0.5 nmol/mouse) + (S)-3,5-DHPG
-  Ifenprodil (2 nmol/mouse) + (S)-3,5-DHPG
-  Ro 25-6981 (2 nmol/mouse) + (S)-3,5-DHPG

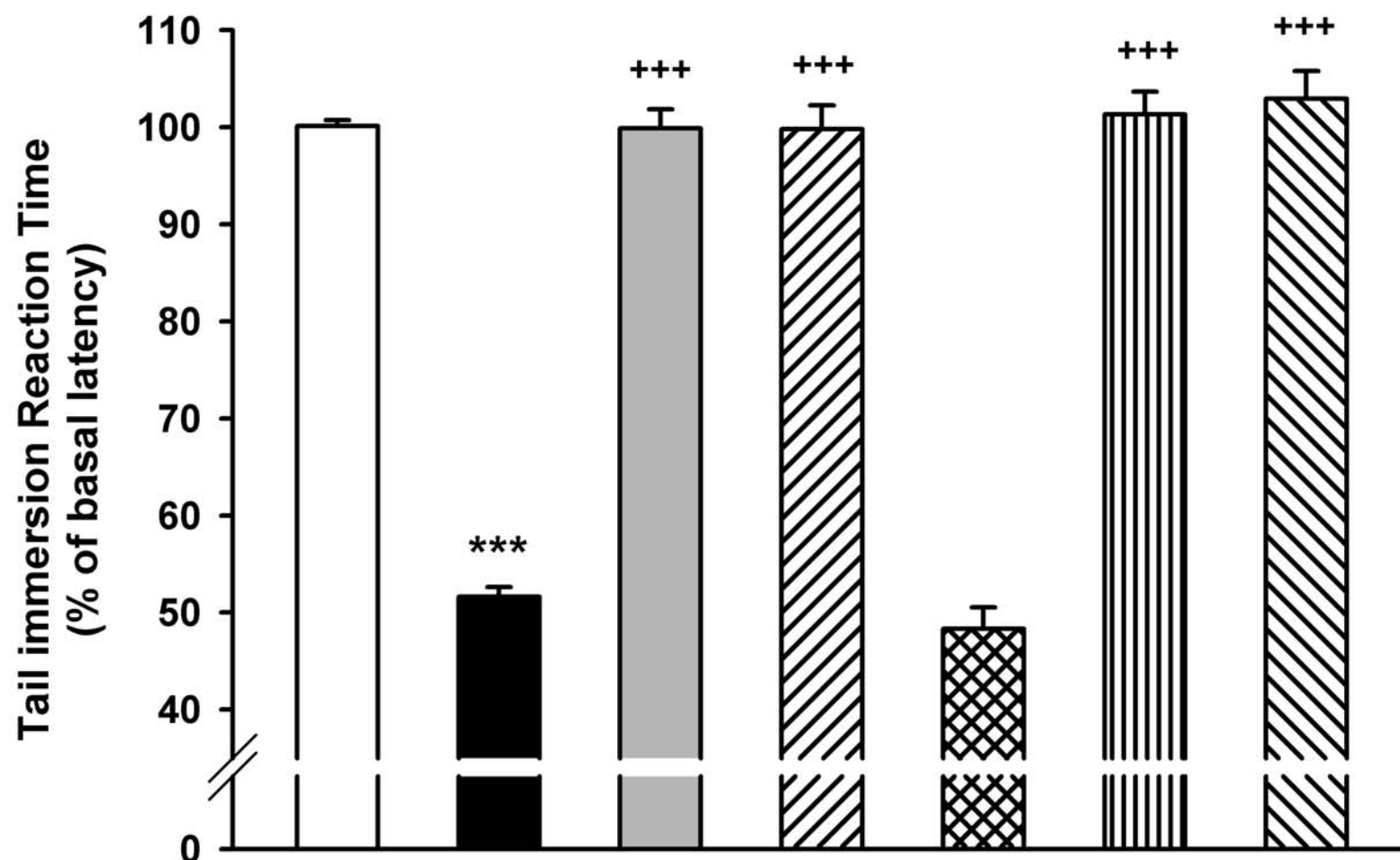
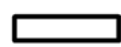







Figure 4

-  Vehicle + Vehicle
-  Vehicle + (*S*)-3,5-DHPG (15 nmol/mouse)
-  Bisindolylmaleimide I (100 pmol/mouse) + (*S*)-3,5-DHPG
-  Go-7874 (2.5 nmol/mouse) + (*S*)-3,5-DHPG
-  PKI-(14-22)-amide (2.5 nmol/mouse) + (*S*)-3,5-DHPG
-  DT-3 (2 nmol/mouse) + (*S*)-3,5-DHPG

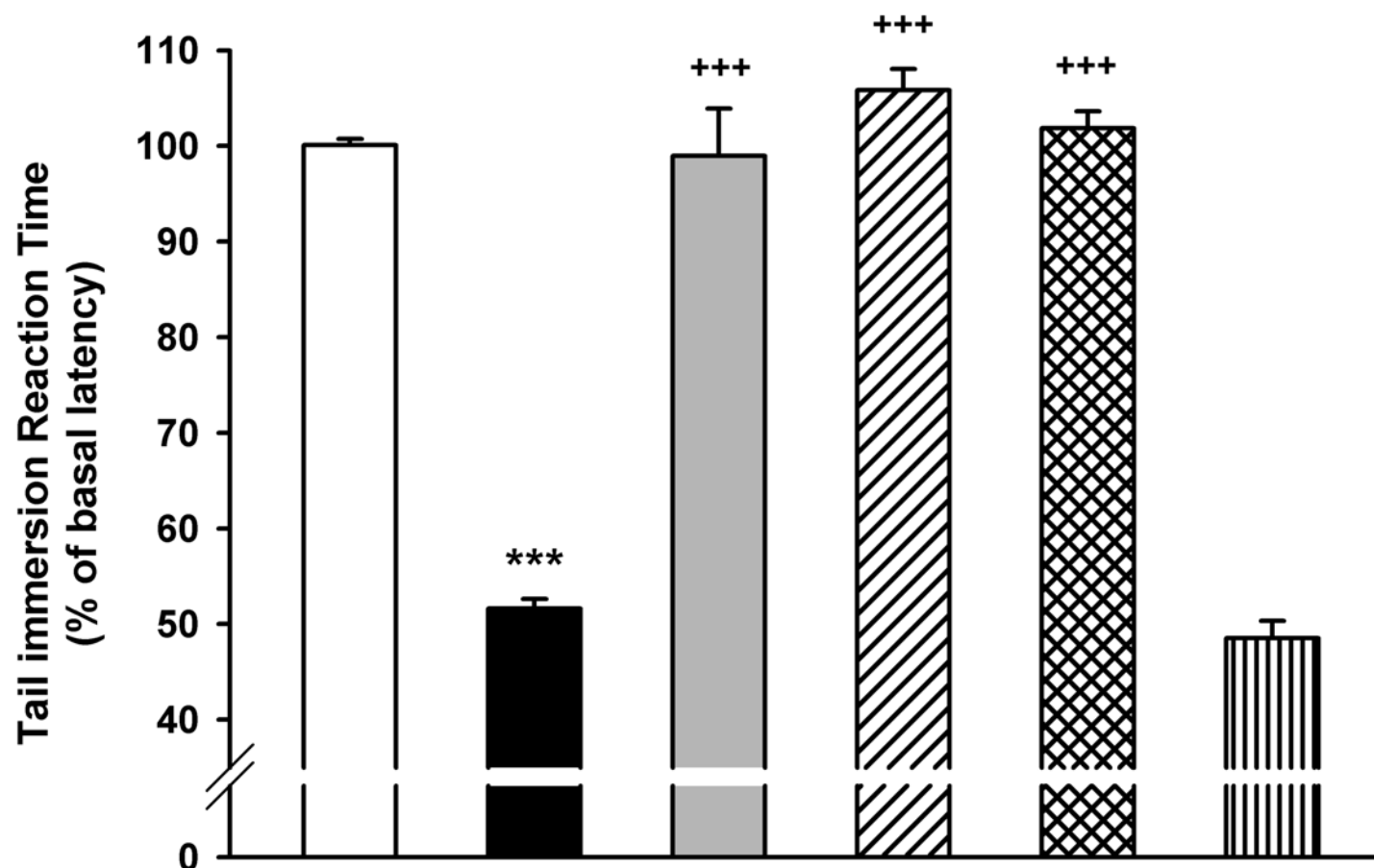






Figure 5

-  Vehicle + Vehicle
-  Vehicle + (S)-3,5-DHPG (15 nmol/mouse)
-  pSM2-NS (1.5 μg/mouse) + (S)-3,5-DHPG
-  pSM2-grin2b (1.5 μg/mouse) + (S)-3,5-DHPG

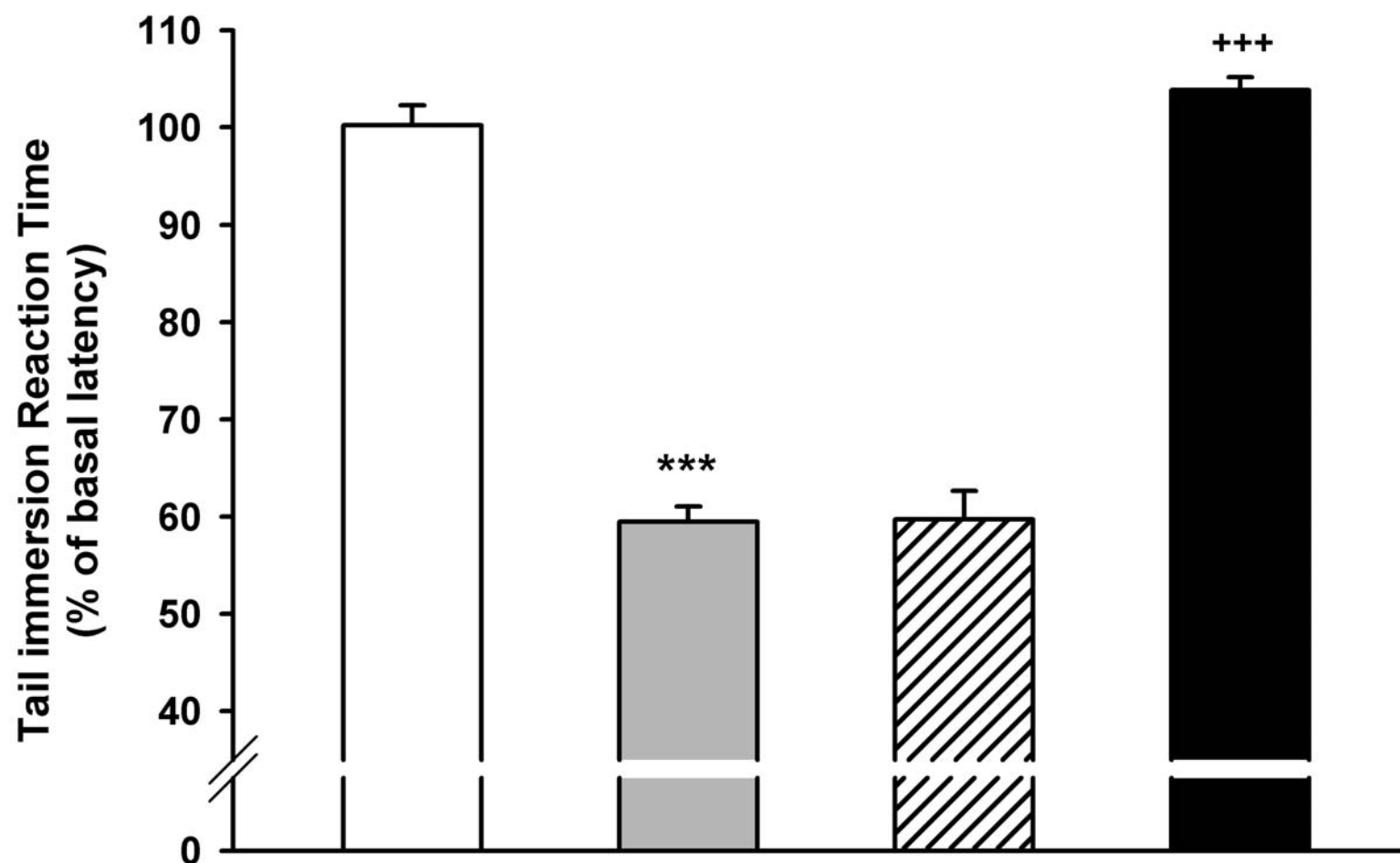


Figure 6

